

Article

Consolidation and Dehydration of Waterlogged Archaeological Wood from Site Huaguangjiao No.1

Xinyou Liu ^{1,2,3,4,*} , Xinwei Tu ², Wanrong Ma ², Changjun Zhang ², Houyi Huang ² and Anca Maria Varodi ^{3,*}

¹ Co-Innovation Center of Efficient Processing and Utilization of Forest Resources, Nanjing Forestry University, Nanjing 210037, China

² College of Furnishing and Industrial Design, Nanjing Forestry University, Str. Longpan No.159, Nanjing 210037, China

³ Faculty of Furniture Design and Wood Engineering, Transilvania University of Braşov, 500036 Braşov, Romania

⁴ Advanced Analysis and Testing Center, Nanjing Forestry University, Str. Longpan No.159, Nanjing 210037, China

* Correspondence: liu.xinyou@njfu.edu.cn (X.L.); anca.varodi@unitbv.ro (A.M.V.); Tel.: +86-25-8542-7408 (X.L.)

Abstract: The Huaguangjiao I is an ancient Chinese wooden shipwreck from the South Song Dynasty (AD 1127–1279) discovered in the South China Sea in 1996. The first phase of its conservation, desalination and desulfurization, was completed in 2016. In this paper, three archaeological wood samples exhibiting different degrees of deterioration from Huaguangjiao No. 1 were consolidated with PEG-4000 and dehydrated via freeze drying and supercritical CO₂ drying methods. The dimensional stability, hygroscopicity, Fourier transform infrared spectroscopy (FTIR), and scanning electron microscopy (SEM) were used to evaluate the effects of consolidation and dehydration. The results showed that PEG4000 was an efficient consolidation material that also effectively decreased shrinkage during dehydration. Furthermore, both vacuum-freeze and supercritical CO₂ drying were efficient methods for treating waterlogged archaeological wood. After PEG4000 impregnation, the shrinkage percentage of the waterlogged archaeological wood became slightly lower than sound wood. The moisture absorption of the experimental specimens ranged within 3.35%–4.53%, and they comprised 50% sound wood, resulting in a marked improvement in dimensional stability. FTIR spectra indicated that impregnation improved wood dimensional stability by reducing hydrophilic groups. These results show that this method can effectively treat waterlogged wood for preservation purposes.

Keywords: dehydration; consolidation; ancient wood; shipwreck; supercritical CO₂ drying; vacuum-freeze drying



Citation: Liu, X.; Tu, X.; Ma, W.; Zhang, C.; Huang, H.; Varodi, A.M. Consolidation and Dehydration of Waterlogged Archaeological Wood from Site Huaguangjiao No.1. *Forests* **2022**, *13*, 1919. <https://doi.org/10.3390/f13111919>

Academic Editor: Magdalena Broda

Received: 20 October 2022

Accepted: 13 November 2022

Published: 15 November 2022

Publisher's Note: MDPI stays neutral with regard to jurisdictional claims in published maps and institutional affiliations.



Copyright: © 2022 by the authors. Licensee MDPI, Basel, Switzerland. This article is an open access article distributed under the terms and conditions of the Creative Commons Attribution (CC BY) license (<https://creativecommons.org/licenses/by/4.0/>).

1. Introduction

Wood is one of the earliest natural materials used by human beings and has been integral to the development of human civilization [1–4]. Ancient wood residues found in soil or water, known as “waterlogged wood”, are important historical materials that represent a significant resource for studying human civilization and culture, serving as chief clues for characterizing the interactions between materials and the environment [5,6]. Waterlogged wood makes up an important part of ancient shipwreck finds, of which more than 50 have been found in China and are of great historical significance to Chinese maritime culture [7,8], most of them made soft wood. Among them, the shipwreck named Huaguangjiao No. 1, dating from the Southern Song Dynasty (AD 1127–1279), was discovered in 1996 near Huaguang Reef in the Xisha Islands, South China Sea. This shipwreck has proven to be an important source for the study of China’s maritime Silk Road during the Southern Song Dynasty [9,10]. In 2008, an archaeological excavation of the underwater site of the ancient ship “Huaguangjiao I” was carried out, and 511 pieces of the wooden

ship were successfully retrieved. The first conservation phase of this ancient shipwreck, involving desalination and desulfurization, was completed in 2016, and the next step will be dehydration, reinforcement, and restoration.

In underground or underwater environments, wood can be preserved for thousands of years in a saturated state. However, wood is susceptible to invasion by degrading microorganisms even under anaerobic conditions, which decompose carbohydrates such as cellulose and hemicellulose and compromise the physical and mechanical properties of the wood [11]. Compared with sound wood, degraded wood is structurally fragile and can exhibit irreversible deformations or cracking during conservation treatments, mainly because the mechanical strength of degraded cell walls is much weaker than the capillary force of evaporating moisture [12–14]. Therefore, consolidation is essential for strengthening deteriorated wood [15]. Generally, the compatibility of the chosen consolidation agent with the wood is extremely important; its composition should not have side effects that alter the properties of the wooden object [6]. Many varieties of additives have been utilized to enhance the wood structures and avoid shrinkage or deformation, including polyethylene glycol [16], polyalkylene glycol [17], grease, polymeric reagents, natural composites [18], and sugars [6,19]. Even though many different consolidation agents have been tested, only a few have been adopted in practice for conservation [20]. Polyethylene glycol (PEG) is inexpensive, non-toxic, user-friendly, and effective at improving dimensional stability, so it has been widely applied in conservation cases, including the Vasa warship [21], Mary Rose [22], and Bremen Cog [23], in addition to numerous other waterlogged wooden objects.

Drying (dehydration) is necessary for the preservation of waterlogged archaeological wood because the presence of water will accelerate the deterioration of the wood and affect its dimensional stability [24]. Compared to sound wood, degradation-related chemical and physical changes in ancient wood cell walls weaken the cells, and degraded cell walls tend to collapse due to capillary forces and the high surface tension of evaporating water, which leads to further deterioration of the wooden structure [14]. Furthermore, waterlogged archaeological wood not only requires drying but also the addition of appropriate reinforcing or protective agents to ensure the strength and dimensional stability of the wood cell walls. Therefore, specialized drying methods are usually applied to waterlogged wood, such as air drying, freeze drying [25], and super-critical CO₂ drying [26–29]. Air drying involves drying at room temperature, wherein the moisture evaporation rate can be adjusted by controlling the air humidity; this is a slow-drying method. Freeze drying, also known as sublimation drying, is a drying process in which wood is frozen to convert water into ice, and then, the ice is sublimated into vapor under a higher vacuum. The process of sublimating water directly into steam prevents the surface tension of water from affecting the wood dimension. Supercritical CO₂ (SuCO₂) fluid has a lower supercritical temperature (31.1 °C) and supercritical pressure (7.38 MPa); it has excellent solubility and heat transfer characteristics and other good properties, such as availability, non-toxicity, non-flammability, high recovery rate, and strong process selectivity. Freeze drying and supercritical CO₂ drying are two common fast-drying methods for waterlogged archaeological wood [30], which provide both calculable logistics and economic advantages while also decreasing the dangers associated with bacterial and fungal growth.

To identify the optimal combination of PEG4000 as a consolidation agent and dehydration methods for wood of the Huaguangjiao No. 1, this study tested the protective effects of hypothetical dehydration and drying methods on archaeological wood from the Huaguangjiao No. 1. Tested properties included moisture absorption, dimensional stability, and mechanical characteristics. The results presented here provide an important reference for the formulation of a secondary protection plan for the wood of the Huaguangjiao No. 1.

2. Materials and Methods

2.1. Materials

Wood species of the “Huaguangjiao I” ancient shipwreck were identified as Chinese white pine (*Pinus armandii*), Scots pine (*Pinus sylvestris*), Chinese cypress (*Cupressus duclouxiana*), Chinese fir (*Cunninghamia* R. Br), and cinnamon wood (*Cinnamomum trew*). In this paper, Scots pine (*Pinus sylvestris*) wood samples with varying degrees of deterioration were extracted from 3 of the 511 plates (length > 5 m, width > 35 cm) obtained from Hainan museum. These plates were water-saturated, with sizes between 5.5 cm and 16.8 cm, with brown and black coloration. The maximum moisture, basic density, acid-insoluble lignin content, and holocellulose content were measured according to the Chinese national standards GB/T1931-2009 [31], GB/T1933-2009 [32], and GB/T2677.6-94 [33] (Table 1). All three sample had maximum moisture values greater than 400%, indicating severe degradation [34]. The samples had a soft texture similar to chocolate, which allowed them to be cut with a microtome knife. For the consolidation and dehydration tests, 10 test specimens 20 mm × 20 mm × 30 mm in size were prepared from each sample.

Table 1. Maximum moisture, basic density, acid-insoluble lignin content, and holocellulose content of three wood samples.

Wood Samples	Maximum Moisture (%)	Basic Density (g/cm ³)	Acid-Insoluble Lignin (%)	Holocellulose (%)
1#	514.64 (40.81) ¹	0.171 (0.007)	59.76 (2.78)	40.67 (1.67)
2#	742.89 (40.55)	0.153 (0.006)	61.45 (1.93)	39.60 (1.09)
3#	1146.45 (70.26)	0.142 (0.005)	62.98 (1.82)	36.60 (1.05)

¹ The data present average values of seven samples (standard deviations in brackets).

2.2. PEG-4000 Impregnation

The 10 specimens from each sample (total 30) were immersed in 70% ethanol for one week, then transferred into 96% ethanol for one week, reducing their moisture contents from their initial levels to 73%–104% (measured as the reduction in ethanol concentration). Subsequently, the specimens were immersed into 20% PEG4000 in a chamber at 60 °C. The concentration of PEG4000 was increased by 5% every 48 h until full saturation, and the dehydration experiment was carried out after 14 days of impregnation.

2.3. Drying Process

Immediately after impregnation, the prepared wood specimens were divided into two groups for vacuum freeze-drying (FD) (five specimens from each sample) and supercritical CO₂-drying (SCD) tests (five specimens from each sample).

The freeze dryer for the vacuum-freeze-drying experiment was the LGJ-10C (Beijing Sihuan Science Instrument Factory Co., Ltd., Beijing, China), the inner diameter of the sealing hood was 200 mm, and the diameter of freezing tray was 180 mm. The specimens were dried at −50 °C for 12 h and then placed in a freeze dryer at 40 °C and 30 Pa. During freeze drying, the water in the specimens can sublimate directly from a solid state to a gaseous state, eliminating any capillary action.

The supercritical CO₂-drying system used in this experiment was the DY221-50-06, which was produced by Nantong HuaAn Supercritical Fluid Extraction Co., Ltd. (Nantong, China). Its structure consists of three parts: a circulating pump, drying adsorption container, CO₂ bottle, and drying containers (5 L and 2 L), as shown in Figure 1. The PEG4000-impregnated specimens were placed in the drying container and sealed. Liquid CO₂ was pumped into the drying container, then the pressure and temperature were increased to 30 MPa and 40 °C for 30 min, saturating the sample with liquid CO₂ before slowly reducing the pressure to the ambient pressure. As the pressure was reduced, the supercritical CO₂ was converted into gas, which carried water with it, removing it from the specimen.

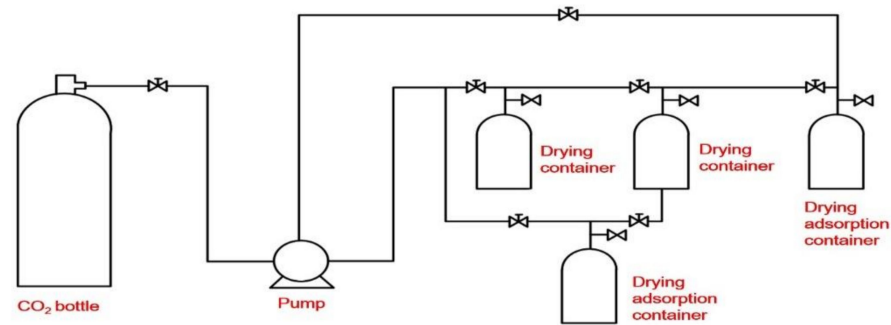


Figure 1. Supercritical CO₂ drying system.

After drying by the two methods, all specimens were placed in an oven at 50 °C and 40% relative humidity to adjust the moisture until reaching equilibrium and weighed.

2.4. Weight Percentage Gain (WPG)

The WPG is calculated from the initial weight and moisture content of the specimen and the mass after PEG4000 impregnation and dehydration, according to Equation (1), as given below:

$$WPG = \frac{w_w - w_0 / (MC - 1)}{w_0 / (MC - 1)} \times 100\% \quad (1)$$

where w_0 is the initial weight of the specimen (g) before impregnation; MC is the maximum moisture from Table 1; and w_w is the weight of the specimen (g) after PEG4000 impregnation and dehydration.

2.5. Shrinkage Percentage (SP)

Wood shrinks when drying and swells as it is absorbing water. When the moisture content of wood is below the fiber saturation point, the water mainly exists in the form of combined water, which is an important factor affecting the wood dimensional. PEG impregnation can effectively reduce shrinkage and prevent cracking during wood drying. The shrinkage percentage is determined based on the dimensions in three directions before and after consolidation and drying according to Equation (2), as shown below:

$$SP = \frac{l_a - l_b}{l_a} \times 100\% \quad (2)$$

where l_a and l_b are the tangential (mm), radial (mm), or longitudinal (mm) dimensions or the volume (mm³), before and after treatment, respectively.

2.6. Estimation of Wood Dimensional Stability

The estimations of wood dimensional stability were based on swelling tests, which were implemented in accordance with GB/T standards 1931–2009. All the immersed and dehydrated specimens were stored at 20 °C with 65% humidity until the moisture content of the specimen reached equilibrium. The swelling coefficient was determined based on the dimensions of specimens before and after conditioning, according to Equation (3) given below:

$$a = \frac{l_w - l_0}{l_0} \times 100\% \quad (3)$$

where a is the swelling coefficient in the tangential (mm), radial (mm), or longitudinal (mm) directions or for the volume (mm³). l_0 is the dimension of specimen before conditioning; l_w is the dimension after consolidation and dehydration.

2.7. Moisture Absorption (MA)

The MA values are determined using the weight of specimens before and after conditioning according to the GB/T 1931–2009 criterions, which is calculated via Equation (4):

$$MA = \frac{w_a - w_b}{w_b} \times 100\% \quad (4)$$

where w_b (w_a) is the specimen weight before (after) conditioning in the climate chamber (g).

2.8. Morphological Characteristic

Morphological observations were performed using a scanning electron microscope (SEM) manufactured by Hitachi S-3400N II, Tokyo, Japan, to evaluate the changes in the microscopic shape and physical structure of the specimens before and after consolidation and dehydration.

2.9. Chemical Structure Analysis Using FTIR Spectroscopy

To illustrate the changes in the chemical structure of degraded and impregnated wood, samples of sound wood of Scots pine (*Pinus sylvestris*), untreated archaeological wood, and PEG 4000-impregnated wood were ground and sieved through an 80-mesh for FTIR investigation. The prepared specimens were collected by direct transmittance using a standard FTIR spectrometer (Tensor 27, Bruker, Germany) through 32 scans at a resolution of 4 cm^{-1} ranging from 700 to 4000 cm^{-1} .

2.10. Statistical Analyses

Consolidation and dehydration effects on waterlogged archaeological wood were investigated based on shrinkage percentage, swelling tests, and moisture absorption. These data were analyzed using two-way ANOVA in the SPSS software (IBM Corporation, IBM SPSS Statistics for Windows, v.25, Armonk, NY, USA) with the probability level set at 0.05. Homogeneity of variance was analyzed using the Levene test, and normality of data was determined using the Shapiro–Wilk test. Fisher’s protected least-significant-difference (LSD) test was used to check for significant differences among treatment means with $\alpha = 0.05$.

3. Results and Discussions

3.1. Weight Percentage Gain (WPG) and Shrinkage Percentage (SP)

WPG is based on the net weight gain of the waterlogged archaeological wood after PEG4000 impregnation, which depends on the permeability of the PEG4000 solution into the wood. Figure 2 presents the results of WPG after consolidation and dehydration. After comparisons of archaeological wood in different deterioration states, the most deteriorated sample (3#) had the largest WPG value (255%–278%), while the WPG of the specimens from the least deteriorated wood sample (1#) was only 107.79%–109.33%. This indicated that while the degradation of cellulose and hemicellulose weakened the cell wall strengths, it also improved the permeability, resulting a better accessibility of the cell walls for PEG4000. Comparing with specimens from FD and SCD groups, dehydration had no significant effect on effect on the weight percentage gain.

Shrinkage is a characteristic of the wood-drying process, whether for sound wood or waterlogged archaeological wood. Wood is an anisotropic material and exhibits different shrinkage percentages in the tangential, radial, and longitudinal directions. According to data from the wood database, the shrinkage percentage of Scots pine in the tangential and radial directions is 8.3% and 5.2%, respectively, and 13.6% in volume, with a tangential/radial shrinkage rate ratio of 1.6. The observed shrinkage percentages of specimens are shown in Figure 3, and after consolidation and dehydration, the shrinkage in the tangential direction was 4.86%–6.21%, in the radial direction was 1.87%–4.16%, and in volume was 7.49%–11.42%, with a tangential/radial shrinkage rate ratio of 1.4–2.6. This revealed that PEG4000 effectively prevented shrinkage of cell walls during drying, resulting in smaller

shrinkage rates in waterlogged archaeological wood than in sound wood. By comparing among the shrinkage ratios of the specimens after treatment by two different dehydration methods, the shrinkage ratio of the specimens treated with vacuum freeze drying was slightly smaller, which may have been because the specimens slightly expanded after 12 h at $-50\text{ }^{\circ}\text{C}$, and their volume decreased very little after sublimation of the solid water. Shrinkage of specimens from samples 2# and 3# was greater than that of specimens from sample 1#, illustrating that specimens with higher degrees of deterioration had higher shrinkage percentages due to their weakened cell walls.

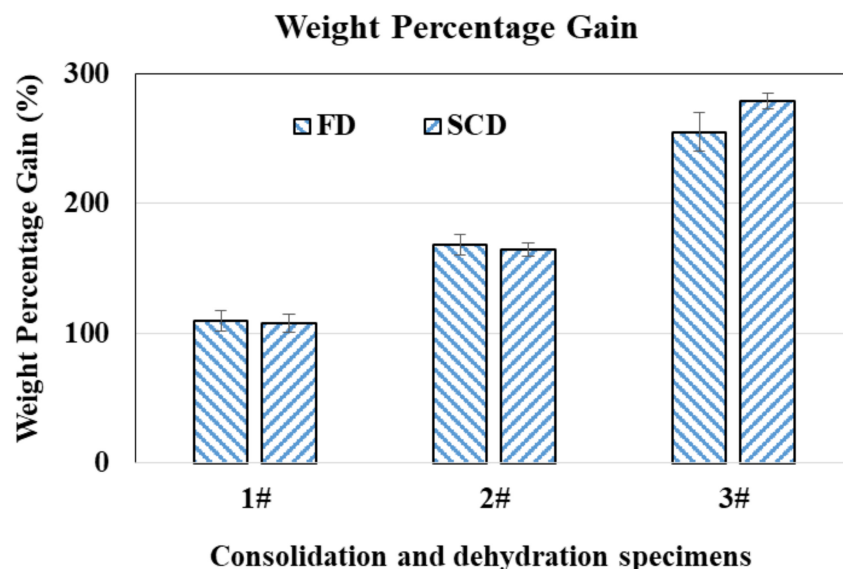


Figure 2. Weight percentage gain of specimens from different samples.

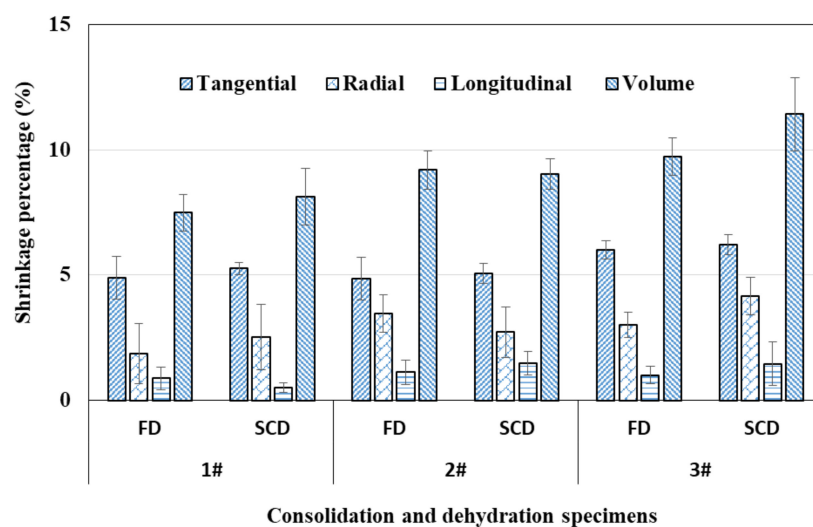


Figure 3. Shrinkage percentage of specimens from different samples.

According to statistical analysis results in Table 2, dehydration method did not significantly affect the shrinkage percentage of the specimens. However, after dehydration, specimens from vacuum freeze drying exhibited slightly less shrinkage. Degree of degradation significantly affected shrinkage in all three directions as well as WPG. Specimens with higher degradation had weaker cell walls, experienced more shrinkage, and took up more PEG4000. The interaction between degradation degree and dehydration method did not significantly affect specimens' shrinkage, with p -values of 0.090–0.931, but did significantly affect WPG.

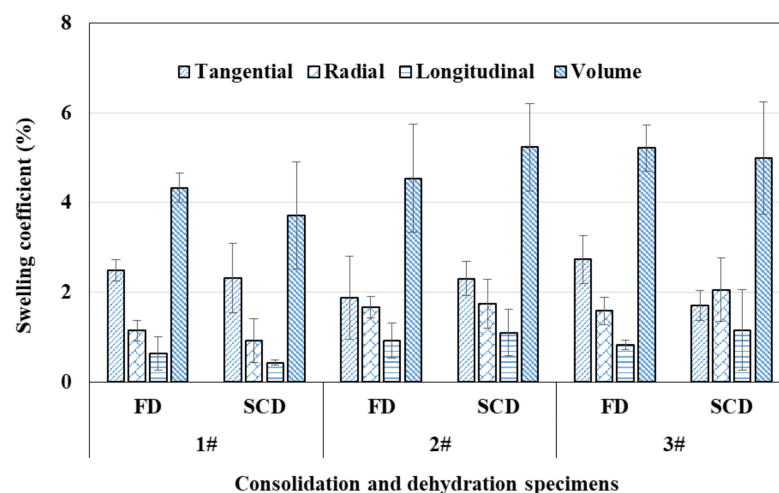
Table 2. Consolidation and dehydration effects on shrinkage percentage and WPG.

Consolidation and Dehydration Effects	Shrinkage Percentage				WPG
	Tangential (%)	Radial (%)	Longitudinal (%)	Volume (%)	
Degradation degree					
1#	5.08 ^b	2.20 ^b	0.69 ^b	7.81 ^c	108.61 ^c
2#	4.97 ^b	3.09 ^a	1.30 ^a	9.11 ^b	166.39 ^b
3#	6.10 ^a	3.58 ^a	1.23 ^a	10.57 ^a	266.50 ^a
Dehydration method					
FD	5.25 ^a	2.78 ^a	1.00 ^a	8.80 ^b	177.46 ^a
SCD	5.52 ^a	3.14 ^a	1.15 ^a	9.52 ^a	183.54 ^a
			<i>p</i> -values		
Degradation degree	<0.0001	0.012	0.027	<0.0001	<0.0001
Dehydration method	0.215	0.315	0.426	0.048	0.071
Degradation degree × dehydration method	0.931	0.090	0.155	0.110	0.003

Note: *p*-values indicate significance of influencing factors. The smaller the *p*-value, the higher the significance. When the *p*-value is less than 0.05, the influencing factor is considered significant, and when the *p*-value is greater than 0.05, it is not significant. The same small superscript letters (^{a,b,c}) within a group are not significantly different based on Fisher's Protected LSD test at the 0.05 significance level.

3.2. Estimation of Wood Dimensional Stability and Moisture Absorption (MA)

Dimensional stability is an important factor for wooden relics since changes in dimensions will lead to deformation or cracking, affecting their preservation and exhibition [35]. The swelling coefficients of specimens from the three wood samples with different degrees of degradation are presented in Figure 4. The swelling coefficients for volume reflect the volumetric swelling (3.71%–5.24%), which was much higher than the swelling coefficients in the tangential, radial, and longitudinal directions. Similarly, the sound wood swelling coefficient in the longitudinal direction (0.43%–1.16%) was much smaller than those in the tangential (1.70%–2.73%) and radial (0.92%–2.06%) directions. Among the swelling coefficients of specimens from different wood samples, the values from sample 3# were higher than those from samples 1# and 2#. There were no significant differences in the swelling coefficients between the two different dehydration methods.

**Figure 4.** Swelling coefficients of specimens from different samples.

Both wood and PEG4000 have absorbent characteristics and absorb moisture in wet conditions, resulting in volume expansion, especially when the wood has not yet reached its fiber saturation point. Under conditions of 50 °C and RH = 40%, the equilibrium moisture content (EMC) of sound wood is about 6.6%, and the EMC of sound wood under 20 °C and RH = 65% is about 11% depending on wood species, sapwood or heartwood,

tree age, and so on. The moisture absorption values of specimens from different samples can be found in Figure 5. All values ranged only between 3.35% and 4.53%, which were similar with sound wood moisture absorption and were smaller than untreated water-logged archaeological wood [30]. This indicated that water absorption by the hydrophilic components was restricted when the degraded wood was impregnated with PEG4000. Clearly, PEG4000 impregnation significantly reduced wood MA and thus enhanced wood dimensional stability.

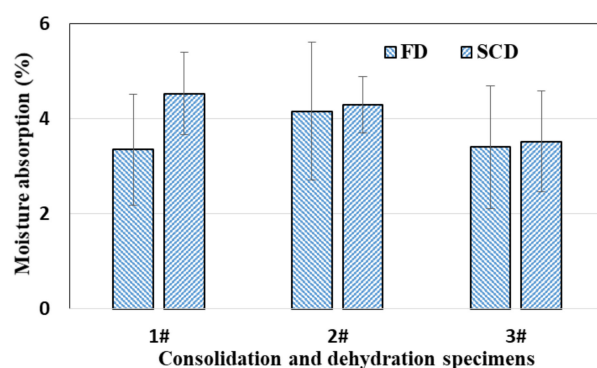


Figure 5. Moisture absorption of specimens from different samples.

According to the experimental results presented in Table 3, the dehydration method did not significantly affect either dimensional stability or moisture absorption of specimens, with p -values between 0.237 and 0.900. The degree of degradation had a significant effect on shrinkage only in the radial and longitudinal directions and in volume, with p -values of 0.001, 0.027, and 0.049. Degradation degree had no significant effect on dimensional stability in the tangential direction or on moisture absorption. The influence of the interaction between degradation degree and dehydration method did not significantly affect specimens' dimensional stability or moisture absorption, with p -values 0.035–0.487.

Table 3. Consolidation and dehydration effects on wood dimensional stability and moisture absorption.

Consolidation and Dehydration Effects	Wood Dimensional Stability				MA
	Tangential (%)	Radial (%)	Longitudinal (%)	Volume (%)	
Degradation degree					
1#	2.41 ^a	1.03 ^b	0.53 ^b	4.02 ^a	3.94 ^a
2#	2.09 ^a	1.71 ^a	1.01 ^a	4.89 ^a	4.22 ^a
3#	2.22 ^a	1.82 ^a	0.99 ^a	5.11 ^a	3.47 ^a
Dehydration method					
FD	2.37 ^a	1.47 ^a	0.79 ^a	4.70 ^a	3.64 ^a
SCD	3.11 ^a	1.57 ^a	0.90 ^a	4.65 ^a	4.12 ^a
			<i>p</i> values		
Degradation degree	0.489	0.001	0.027	0.049	0.315
Dehydration method	0.237	0.529	0.426	0.900	0.246
Degradation degree × dehydration method	0.035	0.245	0.155	0.318	0.478

Note: p -values indicate significance of influencing factors. The smaller the p -value, the higher the significance. When the p -value is less than 0.05, the influencing factor is considered significant, and when the p -value is greater than 0.05, it is not significant. The same small superscript letters (^{a,b}) within a group are not significantly different based on Fisher's Protected LSD test at the 0.05 significance level.

3.3. FTIR Spectroscopy

Figure 6 presents the FTIR spectra of sound wood, sample 3# wood, and a wood specimen immersed in PEG4000. Compared to the spectrum of sound wood, the spectrum of the sample 3# wood had clear differences. There were elevated peaks at around

1730 cm^{-1} related to the C=O tensile vibration of xylan and around 1370 cm^{-1} related to CH deformation (symmetric) in carbo-hydrates, but the peaks belonging to the stretching vibration of the carbon-oxygen double bond of xylan acetyl group ($\text{CH}_3\text{C}=\text{O}$) were tiny or absent, indicating that the cellulose and hemicellulose contents in the waterlogged archaeological wood samples were low [36–38]. In contrast, the peaks at 1598 cm^{-1} corresponding to C=C stretching of the aromatic ring (lignin) [39] were slightly elevated in the deteriorated wood, while the peaks around 1510 cm^{-1} were not much different, indicating that the content of lignin in the ancient wood had increased [40], which meant that the lignin had only slightly degraded during the deterioration process, which was consistent with previous findings [34,41–43]. In the spectra of the PEG4000 immersed wood, the band at 3400 cm^{-1} corresponding to the stretching vibration of hydroxyl (-OH) [44–48] decreased notably; these groups are related to the hydrophilic chemical composition and may be why the dimensional stability was improved.

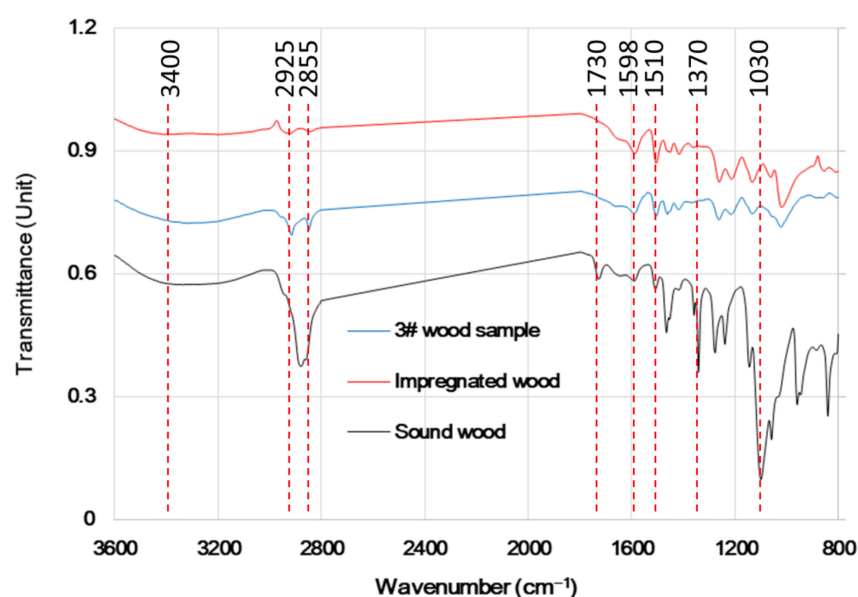


Figure 6. FTIR spectra of the specimens immersed in PEG4000 and those un-impregnated.

3.4. Morphology

SEM micrographs of the specimens in the untreated and impregnated groups are presented in Figure 7. PEG4000 was found to be fully integrated throughout the specimen structure. It was evident that thick PEG4000 had attached to the tracheid walls of the specimens, preventing MA in the conditions in which the archaeological wood was placed, which improved its dimensional stability. PEG4000 could, therefore, reduce MA when it covered intrinsic layers of archaeological wood, thereby enhancing wood dimensional stability.

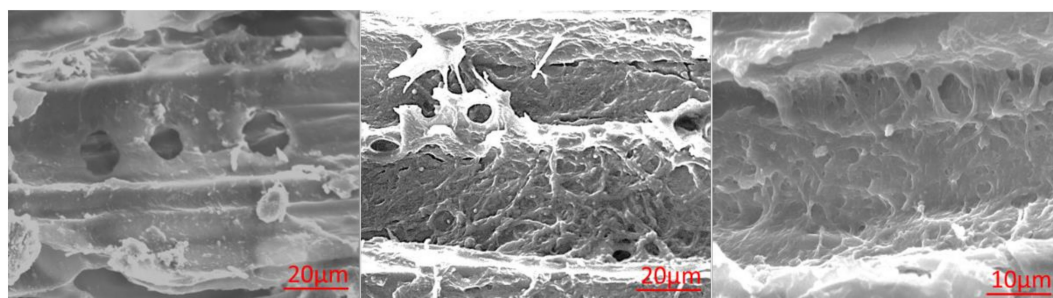


Figure 7. SEM micrographs of the un-impregnated group (left) and the PEG4000 impregnated group (center and right).

4. Conclusions

PEG4000 solution impregnation treatment effectively enhanced the stability of waterlogged archaeological wood and reduced wood shrinkage during dehydration. Under the protection of PEG4000, vacuum freeze drying and supercritical CO₂ drying both proceeded rapidly and were effective dehydration methods for waterlogged archaeological wood. The shrinkage of ancient wood during dehydration was slightly less than that of sound wood. PEG impregnation reduced water absorption in ancient wood to only 3.35 to 4.53%. Under the conditions of 20 °C and RH = 65%, ancient wood absorbed moisture, with a much larger swelling coefficient in the tangential direction than in the radial and longitudinal directions. The degree of deterioration significantly influenced the shrinkage, swelling, and moisture absorption of ancient wood. The FTIR analysis showed that PEG4000 impregnation significantly reduced the hydrophilic groups in ancient wood, which was an important factor in reducing water absorbance and improving stability. SEM images showed that the PEG4000 solution in ancient wood had good accessibility of the cell walls and was uniformly attached throughout the tracheid walls. Therefore, PEG4000 is an effective consolidation and dehydration pre-treatment material for waterlogged archaeological wood.

Author Contributions: X.L. made substantial contributions to the conception and design of the work and the acquisition, analysis, and interpretation of data for the work; X.T., W.M., C.Z. and H.H. carried out the experiments; A.M.V. and X.L. gave valuable suggestions on the experiments and manuscript; X.L. and A.M.V. modified the manuscript in detail. All authors have read and agreed to the published version of the manuscript.

Funding: This work was supported by the Nanjing Forestry University Foundation for Basic Research (Grant No. 163104127) and the Priority Academic Program Development (PAPD) of Jiangsu Province, China.

Data Availability Statement: Not applicable.

Acknowledgments: This work was supported by Hainan museum and the China Scholarship Council (CSC) scholarship under a post-doc program.

Conflicts of Interest: The authors declare no conflict of interest.

References

1. Popescu, C.M.; Tibirna, C.M.; Vasile, C. XPS characterization of naturally aged wood. *Appl. Surf. Sci.* **2009**, *256*, 1355–1360. [[CrossRef](#)]
2. Feng, X.; Chen, J.; Yu, S.; Wu, Z.; Huang, Q. Mild hydrothermal modification of beech wood (*Zelkova schneideriana* Hand-Mzt): Its physical, structural, and mechanical properties. *Eur. J. Wood Prod.* **2022**, *80*, 933–945. [[CrossRef](#)]
3. Sun, G.R.; He, Y.R.; Wu, Z.H. Effects of thermal treatment on the dimensional stability and chemical constituents of new and aged camphorwood. *BioResources* **2022**, *17*, 4186–4195. [[CrossRef](#)]
4. Fu, Y.; Yang, L.; Zhang, M.; Lin, Z.; Shen, Z. Recent advances in cellulose-based polymer electrolytes. *Cellulose* **2022**, *29*, 8997–9034. [[CrossRef](#)]
5. Tahira, A.; Howard, W.; Pennington, E.R.; Kennedy, A. Mechanical strength studies on degraded waterlogged wood treated with sugars. *Stud. Conserv.* **2016**, *62*, 223–226. [[CrossRef](#)]
6. Walsh-Korb, Z.; Averous, L. Recent developments in the conservation of materials properties of historical wood. *Prog. Mater. Sci.* **2019**, *102*, 167–221. [[CrossRef](#)]
7. Xie, B.; Zhu, X.; Grydehøj, A. Perceiving the Silk Road Archipelago: Archipelagic relations within the ancient and 21st Century Maritime Silk Road. *Isl. Stud. J.* **2020**, *15*, 55–72. [[CrossRef](#)]
8. Bao, Q. The application of big data technology in the research of ancient Chinese silk road. *J. Phys. Conf. Ser.* **2020**, *1578*, 012144. [[CrossRef](#)]
9. Chen, Y.; Luo, W.; Li, N.; Wang, C. A study on provenance of marine porcelains from Huaguangjiao No. 1 after sample desalination. *J. Archaeol. Sci. Rep.* **2016**, *5*, 547–556. [[CrossRef](#)]
10. Shen, D.; Li, N.; Fu, Y.; Macchioni, N.; Sozzi, L.; Tian, X.; Liu, J. Study on wood preservation state of Chinese ancient shipwreck Huaguangjiao I. *J. Cult. Herit.* **2018**, *32*, 53–59. [[CrossRef](#)]
11. Han, L.; Guo, J.; Wang, K.; Gronquist, P.; Li, R.; Tian, X.; Yin, Y. Hygroscopicity of waterlogged archaeological wood from Xiaobaijiao No.1 shipwreck related to its deterioration state. *Polymers* **2020**, *12*, 834. [[CrossRef](#)]
12. Ringman, R.; Beck, G.; Pilgard, A. The Importance of Moisture for Brown Rot Degradation of Modified Wood: A Critical Discussion. *Forests* **2019**, *10*, 522. [[CrossRef](#)]

13. Broda, M.; Hill, C.A.S. Conservation of Waterlogged Wood—Past, Present and Future Perspectives. *Forests* **2021**, *12*, 1193. [[CrossRef](#)]
14. Fejfer, M.; Majka, J.; Zborowska, M. Dimensional Stability of Waterlogged Scots Pine Wood Treated with PEG and Dried Using an Alternative Approach. *Forests* **2020**, *11*, 1254. [[CrossRef](#)]
15. Moise, V.; Stanculescu, I.; Vasilca, S.; Cutrubinis, M.; Pincu, E.; Oancea, P.; Raducan, A.; Meltzer, V. Consolidation of very degraded cultural heritage wood artefacts using radiation curing of polyester resins. *Radiat. Phys. Chem.* **2019**, *156*, 314–319. [[CrossRef](#)]
16. Pournou, A. Wood Deterioration by Aquatic Microorganisms. In *Biodeterioration of Wooden Cultural Heritage*; Springer: Berlin/Heidelberg, Germany, 2020; pp. 177–260.
17. Pournou, A.; Moss, S.T.; Jones, A.M. Preliminary studies on polyalkylene glycols (PAGs) as a pre-treatment to the freeze-drying of waterlogged archaeological wood. In Proceedings of the 7th ICOM-CC Working Group on Wet Organic Archaeological Materials Conference, Grenoble, France, 19–23 October 1998; pp. 104–109.
18. Broda, M. Natural Compounds for Wood Protection against Fungi—A Review. *Molecules* **2020**, *25*, 3538. [[CrossRef](#)]
19. Imazu, S.; Morgòs, A. Conservation of waterlogged wood using sugar alcohol and comparison the effectiveness of lactitol, sucrose and PEG 4000 treatment. In Proceedings of the 6th ICOM Group on Wet Organic Archaeological Materials Conference, York, UK, 9–13 September 1996; pp. 235–254.
20. Han, L.; Guo, J.; Tian, X.; Jiang, X.; Yin, Y. Evaluation of PEG and sugars consolidated fragile waterlogged archaeological wood using nanoindentation and ATR-FTIR imaging. *Int. Biodeterior. Biodegrad.* **2022**, *170*, 105390. [[CrossRef](#)]
21. Seborg, R.M.; Inverarity, R.B. Preservation of old, waterlogged wood by treatment with polyethylene glycol. *Science* **1962**, *136*, 649–650. [[CrossRef](#)]
22. Sandstrom, M.; Jalilehvand, F.; Damian, E.; Fors, Y.; Gelius, U.; Jones, M.; Salome, M. Sulfur accumulation in the timbers of King Henry VIII’s warship Mary Rose: A pathway in the sulfur cycle of conservation concern. *Proc. Natl. Acad. Sci. USA* **2005**, *102*, 14165–14170. [[CrossRef](#)]
23. Hoffmann, P.; Singh, A.P.; Kim, Y.S.; Wi, S.G.; Schmitt, U. The Bremen Cog of 1380—An electron microscopic study of its degraded wood before and after stabilization with PEG. *Holzforschung* **2004**, *58*, 211–218. [[CrossRef](#)]
24. Nguyen, T.D.; Sakakibara, K.; Imai, T.; Tsujii, Y.; Kohdzuma, Y.; Sugiyama, J. Shrinkage and swelling behavior of archaeological waterlogged wood preserved with slightly crosslinked sodium polyacrylate. *J. Wood Sci.* **2018**, *64*, 294–300. [[CrossRef](#)]
25. Jones, S.P.; Slater, N.K.; Jones, M.; Ward, K.; Smith, A.D. Investigating the processes necessary for satisfactory freeze-drying of waterlogged archaeological wood. *J. Archaeol. Sci.* **2009**, *36*, 2177–2183. [[CrossRef](#)]
26. Liu, H.; Xie, J.; Zhang, J. Moisture transfer and drying stress of eucalyptus wood during supercritical CO₂ (ScCO₂) dewatering and ScCO₂ combined oven drying. *BioResources* **2022**, *17*, 5116–5128. [[CrossRef](#)]
27. Yang, L. Effect of Temperature and Pressure of Supercritical CO₂ on Dewatering, Shrinkage and Stresses of Eucalyptus Wood. *Appl. Sci.* **2021**, *11*, 8730. [[CrossRef](#)]
28. Yang, L.; Liu, H. Effect of Supercritical CO₂ Drying on Moisture Transfer and Wood Property of Eucalyptus urophydis. *Forests* **2020**, *11*, 1115. [[CrossRef](#)]
29. Zhang, J.-W.; Liu, H.-H.; Yang, H.; Yang, L. Drying Characteristics of *Eucalyptus urophylla* × *E. grandis* with Supercritical CO₂. *Materials* **2020**, *13*, 3989. [[CrossRef](#)]
30. Broda, M.; Curling, S.F.; Frankowski, M. The effect of the drying method on the cell wall structure and sorption properties of waterlogged archaeological wood. *Wood Sci. Technol.* **2021**, *55*, 971–989. [[CrossRef](#)]
31. GB/T 1931; Method for Determination of the Moisture Content of Wood. Standardization Administration of China: Beijing, China, 2009.
32. GB/T 1933; Method for Determination of the Density of Wood. Standardization Administration of China: Beijing, China, 2009.
33. GB/T 2677.6-1994; Fibrous Raw Material. Determination of Solvent Extractives. Standardization Administration of China: Beijing, China, 1994.
34. Gao, J.; Li, J.; Qiu, J.; Guo, M. Degradation assessment of waterlogged wood at Haimenkou site. *Frat. Integratà Strutt.* **2014**, *8*, 495–501.
35. Mori, M.; Kuhara, S.; Kobayashi, K.; Suzuki, S. Nondestructive visualization of polyethylene glycol impregnation in wood using ultrashort echo time 3D imaging. *J. Cult. Herit.* **2021**, *50*, 43–48. [[CrossRef](#)]
36. Gregory, M. Wood identification: An annotated bibliography. *Iawa J.* **1980**, *1*, 3–41. [[CrossRef](#)]
37. Sehlstedt-Persson, S.M.B. High-temperature drying of Scots pine. A comparison between HT-and LT-drying. *Holz als Roh-und Werkstoff* **1995**, *53*, 95–99. [[CrossRef](#)]
38. Derkowski, A.; Mirski, R.; Majka, J. Determination of sorption isotherms of scots pine (*Pinus sylvestris* L.) Wood strands loaded with melamine-urea-phenol-formaldehyde (Mupf) resin. *Wood Res.* **2015**, *60*, 201–210.
39. Sivrikaya, H.; Hosseinpourpia, R.; Ahmed, S.A.; Adamopoulos, S. Vacuum-heat treatment of Scots pine (*Pinus sylvestris* L.) wood pretreated with propanetriol. *Wood Mater. Sci. Eng.* **2022**, *17*, 328–336. [[CrossRef](#)]
40. Han, L.; Tian, X.; Keplinger, T.; Zhou, H.; Li, R.; Svedstrom, K.; Burgert, I.; Yin, Y.; Guo, J. Even visually intact cell walls in waterlogged archaeological wood are chemically deteriorated and mechanically fragile: A case of a 170 Year-old shipwreck. *Molecules* **2020**, *25*, 1113. [[CrossRef](#)]
41. Liu, Y.; Liu, H.; Shen, Z. Nanocellulose Based Filtration Membrane in Industrial Waste Water Treatment: A Review. *Materials* **2021**, *14*, 5398. [[CrossRef](#)]

42. Antonelli, F.; Galotta, G.; Sidoti, G.; Zikeli, F.; Nisi, R.; Davidde Petriaggi, B.; Romagnoli, M. Cellulose and lignin nano-scale consolidants for waterlogged archaeological wood. *Front. Chem.* **2020**, *8*, 32. [[CrossRef](#)]
43. Bjurhager, I.; Halonen, H.; Lindfors, E.L.; Iversen, T.; Almkvist, G.; Gamstedt, E.K.; Berglund, L.A. State of degradation in archeological oak from the 17th century Vasa ship: Substantial strength loss correlates with reduction in (holo) cellulose molecular weight. *Biomacromolecules* **2012**, *13*, 2521–2527. [[CrossRef](#)]
44. Chaochanchaikul, K.; Jayaraman, K.; Rosarpitak, V.; Sombatsompop, N. Influence of lignin content on photodegradation in wood/HDPE composites under UV weathering. *BioResources* **2012**, *7*, 38–55.
45. Jiang, J.; Li, J.; Gao, Q. Effect of flame retardant treatment on dimensional stability and thermal degradation of wood. *Constr. Build. Mater.* **2015**, *75*, 74–81. [[CrossRef](#)]
46. Popescu, M.C.; Jones, D.; Krzysnik, D.; Humar, M. Determination of the effectiveness of a combined thermal/chemical wood modification by the use of FTIR spectroscopy and chemometric methods. *J. Mol. Struct.* **2020**, *1200*, 127–133. [[CrossRef](#)]
47. Timar, M.C.; Tuduce Trăistaru, A.A.; Patachia, S.; Croitoru, C. An investigation of consolidates penetration on wood—Part 2: FTIR Spectroscopy. *ProLigno* **2011**, *7*, 25–38.
48. He, Z.B.; Yang, F.; Wang, Z.Y.; Zhao, Z.J.; Yi, S.L. Reducing wood drying time by application of ultrasound pretreatment. *Dry. Technol.* **2016**, *34*, 1141–1146. [[CrossRef](#)]